

Relativistic calculations of $R(D^{(*)})$, $R(D_s^{(*)})$, $R(\eta_c)$ and $R(J/\psi)$

Tian Zhou,¹ Tianhong Wang², Yue Jiang,³ Xiao-Ze Tan,⁴ Geng Li,⁵ Guo-Li Wang⁶

School of Physics, Harbin Institute of Technology, Harbin 150001, China

ABSTRACT: Recently, the deviation of the ratios $R(D)$, $R(D^*)$ and $R(J/\psi)$ have been found between experimental data and the Standard Model predictions, which may be the hint of New Physics. In this work, we calculate these ratios within the Standard Model by using the improved instantaneous Bethe-Salpeter method. The emphasis is paid to the relativistic correction of the form factors. The results are $R(D) = 0.312^{+0.006}_{-0.007}$, $R(D^*) = 0.249^{+0.001}_{-0.002}$, $R(D_s) = 0.320^{+0.009}_{-0.009}$, $R(D_s^*) = 0.251^{+0.002}_{-0.003}$, $R(\eta_c) = 0.384^{+0.032}_{-0.042}$, and $R(J/\psi) = 0.267^{+0.009}_{-0.011}$, which are consistent with predictions of other models and the experimental data. The semileptonic decay rates and corresponding form factors at zero recoil are also given.

¹tianzhou@hit.edu.cn.

²Corresponding author. thwang@hit.edu.cn.

³jiangure@hit.edu.cn

⁴xz.tan@hit.edu.cn

⁵karlisle@hit.edu.cn

⁶glwang@hit.edu.cn

1 Introduction

As we all believe, the Standard Model (SM) is not a perfect theory especially at higher scale, so it is significant to test SM precisely to search the new physics (NP) beyond SM[1]. Recently, several experiments reported a few anomalous results of $R(D^{(*)})$ and $R(J/\psi)$, which are defined as

$$R(D^{(*)}) = \frac{Br(B \rightarrow D^{(*)}\tau\nu)}{Br(B \rightarrow D^{(*)}\ell\nu)}, \quad (1.1)$$

and

$$R(J/\psi) = \frac{Br(B_c \rightarrow J/\psi\tau\nu)}{Br(B_c \rightarrow J/\psi\mu\nu)}, \quad (1.2)$$

respectively. The research of $R(D^{(*)})$ and $R(J/\psi)$ has become interesting, because people believe these quantities can be used to explore NP [1–13]. Moreover, as the Cabibbo-Kobayashi-Maskawa (CKM) matrix element V_{cb} contained in the branching fractions canceled each other out, the uncertainties originate from them are reduced.

These ratios have been measured by BaBar [14, 15], Belle [16–18], and LHCb [19–21]. The averaging B -tagged measurements of $R(D)$ and $R(D^*)$ at the $\Upsilon(4S)$ and the LHCb measurements of $R(D^*)$ yield [22]

$$\begin{aligned} R(D)^{\text{EX}} &= 0.407 \pm 0.039 \pm 0.024, \\ R(D^*)^{\text{EX}} &= 0.304 \pm 0.013 \pm 0.007. \end{aligned} \quad (1.3)$$

Theoretically, there are already many precise SM predictions of these ratios. For example, by fitting the lattice calculations and recent experimental data, Bigi and Gambino obtained [23]

$$R(D)^{\text{SM}} = 0.299 \pm 0.003. \quad (1.4)$$

For $R(D^*)$, by using the heavy quark expansion and combining with the recent measurements of $\bar{B} \rightarrow D^*\ell\bar{\nu}_\ell$, Fajfer et al. obtained [6]

$$R(D^*)^{\text{SM}} = 0.252 \pm 0.003. \quad (1.5)$$

Flavour Lattice Averaging Group (FLAG) combined recent lattice calculations and gave the average value [24]

$$R(D)^{\text{SM}} = 0.300 \pm 0.008. \quad (1.6)$$

We can easily see that the experimental values of $R(D)$ and $R(D^*)$ deviate from the SM predictions by 2.3σ and 3.4σ [22], respectively.

Most recently, LHCb reported the ratio of branching fractions [25]

$$R(J/\psi)^{\text{EX}} = \frac{Br(B_c \rightarrow J/\psi\tau\nu)}{Br(B_c \rightarrow J/\psi\mu\nu)} = 0.71 \pm 0.17 \pm 0.18. \quad (1.7)$$

The SM predictions lie in the range $R(J/\psi) \in [0.23, 0.29]$, from which the data deviate by 2σ . To account for this deviation, both the new physics scenarios and the systematic errors were considered [26–28].

The deviations of $R(D^{(*)})$ and $R(J/\psi)$ have motivated lots of theoretical studies on the semi-leptonic decays of $B_{(s)}$ to S -wave charmed mesons. Besides papers mentioned above, the $B \rightarrow D(D^*)$ decays have been studied by QCD sum rules [29–31], constituent quark models [32], Lattice QCD in the framework of heavy quark effective theory (HQET) [33, 34], and HQET method with the $O(\alpha_s, \Lambda_{\text{QCD}}/m_{b,c})$ and (part of) the $O(\Lambda_{\text{QCD}}^2/m_c^2)$ corrections [35], etc.

For the $B_c \rightarrow J/\psi(\eta_c)$ transitions, many other approaches, such as perturbative QCD (PQCD) [36], QCD sum rules (QCDSR) [37], light-cone QCD sum rules (LCSR) [38, 39], nonrelativistic QCD (NRQCD) [40, 41], the covariant light-front quark model (CLFQM) [42], the nonrelativistic quark model (NRQM) [43], the relativistic quark model model (RQM) [44], the covariant confined quark model (CCQM) [27] etc, have been used.

To explain the deviations, a lot of new physics models [4, 7–13] have been proposed. However, to make a reliable prediction of the NP, one needs both detections and theoretical calculations within the SM with more precision to study these observables $R(D^{(*)})$ and $R(J/\psi)$. For example, recently, the Belle collaboration presented an updated measurement of $R(D)$ which is $0.307 \pm 0.037 \pm 0.016$ [45]. It is in agreement with the SM prediction within 0.2σ .

In this work, we will give a relativistic study of $R(D^{(*)})$ and $R(J/\psi)$ by using the improved instantaneous Bethe-Salpeter (BS) method. One of the essential parts of this method is the instantaneous BS wave function (also called Salpeter wave function) of mesons, which is achieved by solving the instantaneous BS equation (also called Salpeter equation). These functions are applied to calculate the hadronic transition matrix element. In our previous work [46], a similar method is used to study the channel $B \rightarrow D(D^*)$, where the results are not quite consistent with the experimental values. One possible reason is that we made approximations when boosting the wave functions of the final mesons to the initial meson rest frame. This method is improved in our another work [47] to study the rare decays of B_c meson. Here we will systematically use this improved BS method to calculate the semi-leptonic decays of B_q and B_c mesons, and make more reliable predictions of $R(D^{(*)})$ and $R(J/\psi)$. Besides that, we will also give other quantities, including form factors, $\mathcal{G}(1)$, the slope ρ^2 , differential decay rate, branching ratios, etc.

The paper is organized as follows. In Section 2, we present the definitions of form factors of different decay channels and the differential decay width. In Section 3, we use the improved BS method to calculate the form factors. In Section 4, we give the numerical results, including the form factors, differential decay rate, partial decay widths, and the ratio of branching fractions. A conclusion is given finally.

2 Formalism of semi-leptonic decays

In this section, we will present the formula of a B_q ($q = u, d, s, c$) meson semi-leptonic decays to a charmed meson with the improved BS method. Fig.1 is the Feynman diagram of the semileptonic decay $B \rightarrow D_q l \bar{\nu}$, whose amplitude is written as

$$T = \frac{G_F}{\sqrt{2}} V_{bc} \bar{u}_\ell \gamma^\mu (1 - \gamma_5) v_{\bar{\nu}_\ell} \langle D_q | J_\mu | B_q \rangle, \quad (2.1)$$

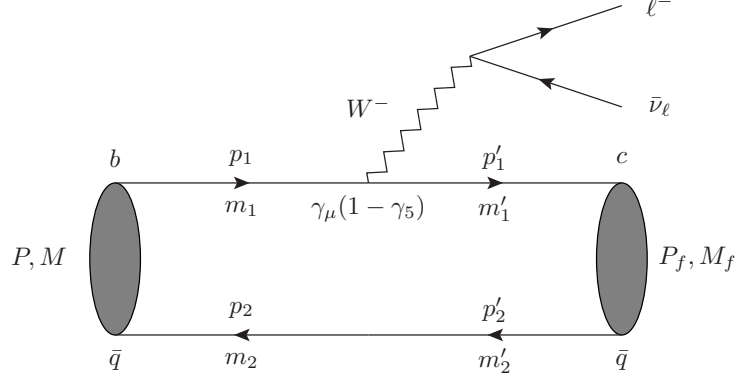


Figure 1: Feynman diagram of the semileptonic B_q decays to a charmed $D_q^{(*)}$ ($q = u, d, s$).

where G_F is the Fermi coupling constant, V_{bc} is the CKM matrix element, $J_\mu = V_\mu - A_\mu$ is the charged electroweak current.

The hadronic matrix element $\langle D_q^{(*)} | (V_\mu - A_\mu) | B_q^- \rangle$ can be characterized by the corresponding form factors. If the final meson is a pseudoscalar state, the matrix element can be written as

$$\begin{aligned}
\langle D_q | V^\mu | B_q \rangle &= F_+(Q^2)(P^\mu + P_f^\mu) + F_-(Q^2)(P^\mu - P_f^\mu) \\
&= F_+(Q^2)(P^\mu + P_f^\mu) + F_-(Q^2)Q^\mu \\
&= f_1(Q^2)(P^\mu + P_f^\mu - \frac{M^2 - M_f^2}{Q^2}Q^\mu) + f_0(Q^2)\frac{M^2 - M_f^2}{Q^2}Q^\mu, \\
\langle D_q | A_\mu | B_q \rangle &= 0,
\end{aligned} \tag{2.2}$$

where P and P_f are the momenta of the initial and final mesons with masses M and M_f , respectively; the definition $Q^\mu = P^\mu - P_f^\mu$ is used; $f_1(Q^2)$, $f_0(Q^2)$ are the form factors which are related to the functions $F_+(Q^2)$ and $F_-(Q^2)$ by

$$f_1(Q^2) = F_+(Q^2), \quad f_0(Q^2) = F_+(Q^2) + \frac{Q^2}{M^2 - M_f^2}F_-(Q^2). \tag{2.3}$$

If the final meson is a vector state, the matrix element is written as

$$\begin{aligned}
\langle D_q^* | V_\mu | B_q \rangle &= ig(Q^2)\varepsilon^{\mu\nu\alpha\tau}\epsilon_\nu P_{f\alpha}P_\tau = \frac{2iV(Q^2)}{M + M_f}\varepsilon^{\mu\nu\alpha\tau}\epsilon_\nu P_{f\alpha}P_\tau, \\
\langle D_q^* | A_\mu | B_q \rangle &= f(Q^2)\epsilon^\mu + a_+(Q^2)(\epsilon \cdot q)(P^\mu + P_f^\mu) + a_-(Q^2)(\epsilon \cdot q)Q^\mu \\
&= 2M_f A_0(Q^2)\frac{\epsilon \cdot q}{Q^2}Q^\mu + (M + M_f)A_1(Q^2)[\epsilon^\mu - \frac{\epsilon \cdot q}{Q^2}Q^\mu] \\
&\quad - A_2(Q^2)\frac{\epsilon \cdot q}{M + M_f}[P^\mu + P_f^\mu - \frac{M^2 - M_f^2}{Q^2}Q^\mu],
\end{aligned} \tag{2.4}$$

where ϵ^μ is the polarization vector of final meson D_q^* ; $\varepsilon^{\mu\nu\alpha\tau}$ is the totally antisymmetric Levi-Civita tensor; $V(Q^2)$, $A_0(Q^2)$, $A_1(Q^2)$, $A_2(Q^2)$ are the form factors which are related to the functions $f(Q^2)$, $a_+(Q^2)$, $a_-(Q^2)$, $v(Q^2)$ by

$$\begin{aligned} V(Q^2) &= \frac{M + M_f}{2} g(Q^2), \quad A_1(Q^2) = -\frac{f(Q^2)}{M + M_f}, \quad A_2(Q^2) = (M + M_f) a_+(Q^2) \\ A_0(Q^2) &= -\frac{1}{2M_f} (Q^2 a_-(Q^2) + f(Q^2) + (M^2 - M_f^2) a_+(Q^2)). \end{aligned} \quad (2.5)$$

The square of the transition amplitude can be written as

$$\sum |T|^2 = \frac{G_F^2}{2} |V_{bc}|^2 L_{\mu\nu} H^{\mu\nu}, \quad (2.6)$$

where we have summed up the possible polarization of final state. $L_{\mu\nu}$ is the leptonic tensor, which has the form

$$\begin{aligned} L_{\mu\nu} &\equiv \bar{u}_\ell \gamma_\mu (1 - \gamma_5) v_{\bar{\nu}_\ell} \bar{v}_{\bar{\nu}_\ell} (1 + \gamma_5) \gamma_\nu u_\ell \\ &= 8 (P_{l\mu} P_{\bar{\nu}\nu} + P_{\bar{\nu}\mu} P_{l\nu} - g_{\mu\nu} P_l \cdot P_{\bar{\nu}} - i \epsilon_{\mu\nu\rho\sigma} P_l^\rho P_{\bar{\nu}}^\sigma), \end{aligned} \quad (2.7)$$

where P_l and $P_{\bar{\nu}}$ are the momenta of l and $\bar{\nu}$, respectively. The hadronic tensor $H^{\mu\nu}$ can be written as

$$\begin{aligned} H^{\mu\nu} &\equiv \sum \langle D_q | J^\mu | B_q \rangle \langle B_q | J^\nu | D_q \rangle \\ &= -\alpha g^{\mu\nu} \\ &\quad + \beta_{++} (P + P_f)^\mu (P + P_f)^\nu + \beta_{+-} (P + P_f)^\mu (P - P_f)^\nu \\ &\quad + \beta_{-+} (P - P_f)^\mu (P + P_f)^\nu + \beta_{--} (P - P_f)^\mu (P - P_f)^\nu \\ &\quad + i \gamma \epsilon^{\mu\nu\rho\sigma} (P + P_f)_\rho (P - P_f)_\sigma, \end{aligned} \quad (2.8)$$

where the functions α , β_{++} , β_{+-} , β_{-+} , β_{--} and γ directly relate to the form factors. For the decays when the final state is a 0^- meson, we have

$$\begin{aligned} \alpha &= \gamma = 0, \\ \beta_{++} &= F_+^2, \quad \beta_{--} = F_-^2, \\ \beta_{+-} &= F_+ F_-, \quad \beta_{-+} = F_- F_+. \end{aligned} \quad (2.9)$$

When the final state is a 1^- meson, the relations are

$$\begin{aligned} \alpha &= f^2 + 4M^2 g^2 |\vec{P}_f|^2, \\ \beta_{++} &= \frac{f^2}{4M_f^2} - M^2 g^2 y + \frac{1}{2} \left[\frac{M^2}{M_f^2} (1 - y) - 1 \right] f a_+ + \frac{M^2 |\vec{P}_f|^2}{M_f^2} a_+^2, \\ \beta_{+-} &= \beta_{-+} = g^2 (M^2 - M_f^2) - \frac{f^2}{4M_f^2} - \frac{1}{2} f (a_+ + a_-) - \frac{1}{2} (a_+ - a_-) \frac{M E_f}{M_f^2} + a_+ a_- \frac{M^2 |\vec{P}_f|^2}{M_f^2}, \\ \beta_{--} &= -g^2 (M^2 + 2M E_f + M_f^2) + \frac{f^2}{4M_f^2} - f a_- \left(\frac{M E_f}{M_f^2} \right) + a_-^2 \frac{M^2 |\vec{P}_f|^2}{M_f^2}, \\ \gamma &= 2g f. \end{aligned} \quad (2.10)$$

Finally, the decay width Γ is read as

$$\Gamma = \frac{1}{2M(2\pi)^9} \int \frac{d^3\vec{P}_f}{2E_f} \frac{d^3\vec{P}_\ell}{2E_\ell} \frac{d^3\vec{P}_{\bar{\nu}}}{2E_{\bar{\nu}}} (2\pi)^4 \delta^4(P - P_f - P_\ell - P_{\bar{\nu}}) \sum |T|^2, \quad (2.11)$$

where E_f , E_ℓ and $E_{\bar{\nu}}$ the energies of $D_q^{(*)}$, ℓ and $\bar{\nu}_\ell$, respectively. By introducing the symbols $x \equiv E_\ell/M$, $y \equiv (P - P_f)^2/M^2$, the differential decay width can be written as

$$\begin{aligned} \frac{d^2\Gamma}{dxdy} = & |V_{cs}|^2 \frac{G_F^2 M^5}{64\pi^3} \left\{ \frac{2\alpha}{M^2} \left(y - \frac{m_\ell^2}{M^2} \right) \right. \\ & + \beta_{++} \left[4 \left(2x \left(1 - \frac{M_f^2}{M^2} + y \right) - 4x^2 - y \right) + \frac{m_\ell^2}{M^2} \left(8x + 4\frac{M_f^2}{M^2} - 3y - \frac{m_\ell^2}{M^2} \right) \right] \\ & + (\beta_{+-} + \beta_{-+}) \frac{m_\ell^2}{M^2} \left(2 - 4x + y - 2\frac{M_f^2}{M^2} + \frac{m_\ell^2}{M^2} + \beta_{--} \frac{m_\ell^2}{M^2} \left(y - \frac{m_\ell^2}{M^2} \right) \right) \\ & \left. - \left[2\gamma y \left(1 - \frac{M_f^2}{M^2} - 4x + y + \frac{m_\ell^2}{M^2} \right) + 2\gamma \frac{m_\ell^2}{M^2} \left(1 - \frac{M_f^2}{M^2} \right) \right] \right\}. \end{aligned} \quad (2.12)$$

And the decay width is

$$\Gamma = \int dx \int dy \frac{d^2\Gamma}{dxdy}. \quad (2.13)$$

3 The improved BS method

The matrix element $\langle D_q^{(*)} | J_\mu | B_q^- \rangle$ will be calculated by the improved BS method. Within Mandelstam formalism, it can be written as

$$\begin{aligned} \langle P_f | J^\mu | P \rangle &= \int \frac{d^4q}{(2\pi)^4} \frac{d^4q_f}{(2\pi)^4} \text{Tr} [\bar{\chi}(P_f, q_f) \Gamma^\mu \chi(P, q) S_2^{-1}(-p_2)] (2\pi)^4 \delta^4(p_2 - p_{2f}) \\ &= \int \frac{d^4q}{(2\pi)^4} \text{Tr} [\bar{\chi}(P_f, q_f) \Gamma^\mu \chi(P, q) S_2^{-1}(-p_2)] \Big|_{q_f = q + \alpha_{2f} P_f - \alpha_2 P} \end{aligned} \quad (3.1)$$

where $\chi(P, q)$ and $\bar{\chi}(P, q)$ are the BS wave function of the initial meson and final meson, respectively, and the latter one has the form $\bar{\chi}(P_f, q_f) = \gamma_0 \chi(P_f, q_f)^\dagger \gamma_0$ in its rest frame; the vertex is $\Gamma^\mu = \gamma^\mu(1 - \gamma^5)$; S_1 and S_2 are propagators of the quark and anti-quark, respectively. q and q_f are the relative momenta of the quark and antiquark within the initial meson. p_1, p_2 are respectively the momenta of the quark and anti-quark within the initial meson, which are related to P and q by

$$p_i = \alpha_i P + J q, \quad \alpha_i \equiv \frac{m_i}{m_1 + m_2}, \quad (3.2)$$

where m_1, m_2 are the masses of the quark and anti-quark, respectively; $J = 1$ and -1 for the cases $i = 1$ and 2 , respectively. For the final meson, we define similar relations

$$p_{if} = \alpha_{if} P_f + J q_f, \quad \alpha_{if} \equiv \frac{m_{if}}{m_{1f} + m_{2f}}. \quad (3.3)$$

The BS wave functions fulfill the BS equation which has the form [48]

$$(\not{p}_1 - m_1)\chi(P, q)(\not{p}_2 + m_2) = i \int \frac{d^4 k}{(2\pi)^4} V(P, k, q)\chi(P, k), \quad (3.4)$$

where $V(P, k, q)$ is the interaction kernel. If we take the instantaneous approximation, the kernel can be reduced to $V(|\vec{q} - \vec{k}|)$. Now we can introduce two 3-dimensional quantities

$$\varphi(q_\perp) \equiv i \int \frac{dq_P}{2\pi} \chi(P, q), \quad \eta(P, q_\perp) \equiv \int \frac{dk_\perp^3}{(2\pi)^3} V(k_\perp, q_\perp) \varphi(k_\perp). \quad (3.5)$$

where we have used the definitions

$$q_P = \frac{P \cdot q}{M}, \quad q_\perp^\mu = q^\mu - q_P P^\mu. \quad (3.6)$$

Then the BS equation can be rewritten as

$$\chi(P, q) = S_1(p_1) \eta(P, q_\perp) S_2(-p_2). \quad (3.7)$$

Using above equations, we can write Eq. (3.1) as

$$\begin{aligned} \langle P_f | J^\mu | P \rangle &= \int \frac{d^4 q}{(2\pi)^4} \text{Tr} [\bar{\eta}(P_f, q_{f\perp}) S_1(p_{1f}) \Gamma^\mu S_1(p_1) \eta(P, q_\perp) S_2(-p_2)] \\ &= \int \frac{d^4 q}{(2\pi)^4} \text{Tr} \left[\frac{\not{P}_f}{M_f} (\tilde{\Lambda}_1^+(p_{1f\perp}) + \tilde{\Lambda}_1^-(p_{1f\perp})) \bar{\eta}(P_f, q_{f\perp}) (\tilde{\Lambda}_2^+(p_{2f\perp}) \right. \\ &\quad \left. + \tilde{\Lambda}_2^-(p_{2f\perp})) \frac{\not{P}_f}{M_f} S_1(p_{1f}) \Gamma^\mu S_1(p_1) \eta(P, q_\perp) S_2(-p_2) \right] \\ &\approx \int \frac{d^4 q}{(2\pi)^4} \text{Tr} \left[\frac{\not{P}_f}{M_f} \tilde{\Lambda}_1^+(p_{1f\perp}) \bar{\eta}(P_f, q_{f\perp}) \tilde{\Lambda}_2^+(p_{2f\perp}) \frac{\not{P}_f}{M_f} \right. \\ &\quad \left. \times S_1(p_{1f}) \Gamma^\mu S_1(p_1) \eta(P, q_\perp) S_2(-p_2) \right]. \end{aligned} \quad (3.8)$$

In the first line of the above equation, we have used Eq. (3.7) with the definition $q_{f\perp} \equiv q_f - \frac{P_f \cdot q_f}{M_f^2} P_f$ for the final meson; in the second line, we have defined the projection operator of the final meson

$$\tilde{\Lambda}_i^\pm(p_{if\perp}) = \frac{1}{2\tilde{\omega}_{if}} \left[\frac{\not{P}_f}{M_f} \tilde{\omega}_{if} \pm (Jm_{if} + \not{p}_{if\perp}) \right], \quad (3.9)$$

with

$$\tilde{\omega}_{if} \equiv \sqrt{m_{if}^2 - p_{if\perp}^2} = \sqrt{m_{if}^2 - q_{f\perp}^2}. \quad (3.10)$$

The relation $\frac{\not{P}_f}{M_f} = \tilde{\Lambda}_1^+(p_{1f\perp}) + \tilde{\Lambda}_1^-(p_{1f\perp})$ is also applied. In the last equation, we have omitted the contribution of the negative energy part, which is very small compared with that of the positive energy part.

Next, we express the propagators $S_i(Jp_i)$ and $S_i(Jp_{if})$ also in terms of the projection operators,

$$\begin{aligned} S_i(Jp_i) &= \frac{\Lambda_i^+(p_{i\perp})}{p_{iP} - \omega_i + i\epsilon} + \frac{\Lambda_i^-(p_{i\perp})}{p_{iP} + \omega_i - i\epsilon}, \\ S_i(p_{if}) &= \frac{\Lambda_i^+(p_{if\perp})}{p_{ifP} - \omega_{if} + i\epsilon} + \frac{\Lambda_i^-(p_{if\perp})}{p_{ifP} + \omega_{if} - i\epsilon}, \end{aligned} \quad (3.11)$$

where

$$\begin{aligned}\Lambda_i^\pm(p_{i\perp}) &= \frac{1}{2\omega_i} \left[\frac{\not{P}}{M} \omega_i \pm (Jm_i + \not{p}_{i\perp}) \right], \quad \omega_i \equiv \sqrt{m_i^2 - p_{i\perp}^2} = \sqrt{m_i^2 - q_\perp^2}, \\ \Lambda_i^\pm(p_{if\perp}) &= \frac{1}{2\omega_{if}} \left[\frac{\not{P}}{M} \omega_{if} \pm (Jm_i + \not{p}_{if\perp}) \right], \quad \omega_{if} \equiv \sqrt{m_{if}^2 - p_{if\perp}^2}.\end{aligned}\tag{3.12}$$

Then Eq. (3.8) can be written as

$$\begin{aligned}\langle P_f | J^\mu | P \rangle &= \int \frac{d^4 q}{(2\pi)^4} \text{Tr} \left[\frac{\not{P}_f}{M_f} \tilde{\Lambda}_1^+(p_{1f\perp}) \bar{\eta}(P_f, q_{f\perp}) \tilde{\Lambda}_2^+(p_{2f\perp}) \frac{\not{P}_f}{M_f} \Lambda_1^+(p_{1f\perp}) \Gamma^\mu \Lambda_1^+(p_{1\perp}) \right. \\ &\quad \left. \times \eta(P, q_\perp) \Lambda_2^+(p_{2\perp}) \right] \frac{1}{(p_{1fP} - \omega_{1f} + i\epsilon)(p_{1P} - \omega_1 + i\epsilon)(p_{2P} - \omega_2 + i\epsilon)},\end{aligned}\tag{3.13}$$

where the quantities p_{1P} , p_{2P} , and p_{1fP} in the denominator are related to q_P by

$$\begin{aligned}p_{1P} &= q_P + \alpha_1 M, \\ p_{2P} &= -q_P + \alpha_2 M, \\ p_{1fP} &= q_P + P_{fP} - \alpha_2 M.\end{aligned}\tag{3.14}$$

By integrating out q_P around the upper plane, we get

$$\begin{aligned}\langle P_f | J^\mu | P \rangle &= -i \int \frac{d\vec{q}}{(2\pi)^3} \text{Tr} \left[\frac{\not{P}_f}{M_f} \tilde{\Lambda}_1^+(p_{1f\perp}) \bar{\eta}(P_f, q_{f\perp}) \tilde{\Lambda}_2^+(p_{2f\perp}) \frac{\not{P}_f}{M_f} \Lambda_1^+(p_{1f\perp}) \Gamma^\mu \right. \\ &\quad \left. \times \Lambda_1^+(p_{1\perp}) \eta(P, q_\perp) \Lambda_2^+(p_{2\perp}) \right] \frac{1}{(P_{fP} - \omega_2 - \omega_{1f})} \frac{1}{(M - \omega_2 - \omega_1)}.\end{aligned}\tag{3.15}$$

The 3-dimensional wave functions (Salpeter wave function) of the initial and final mesons fulfill corresponding Salpeter equations

$$\begin{aligned}\varphi^{++}(P, q_\perp) &= \frac{\Lambda_1^+(p_{1\perp}) \eta(P, q_\perp) \Lambda_2^+(p_{2\perp})}{M - \omega_1 - \omega_2}, \\ \varphi^{++}(P_f, q_{f\perp}) &= \frac{\tilde{\Lambda}_1^+(p_{1f\perp}) \eta(P_f, q_{f\perp}) \tilde{\Lambda}_2^+(p_{2f\perp})}{M_f - \tilde{\omega}_{1f} - \tilde{\omega}_{2f}},\end{aligned}\tag{3.16}$$

where we have used the definitions

$$\begin{aligned}\varphi^{++}(P, q_\perp) &= \Lambda_1^+(p_{1\perp}) \frac{\not{P}}{M} \varphi(P, q_\perp) \frac{\not{P}}{M} \Lambda_2^+(p_{2\perp}), \\ \varphi^{++}(P_f, q_{f\perp}) &= \tilde{\Lambda}_1^+(p_{1f\perp}) \frac{\not{P}_f}{M_f} \varphi(P_f, q_{f\perp}) \frac{\not{P}_f}{M_f} \tilde{\Lambda}_2^+(p_{2f\perp}),\end{aligned}\tag{3.17}$$

whose explicit form can be found in Eq.(3.20) and Eq.(3.22). Then the hadronic transition matrix element is written as [47]

$$\langle P_f | J^\mu | P \rangle = -i \int \frac{d\vec{q}}{(2\pi)^3} \text{Tr} \left[\frac{\not{P}_f}{M_f} \bar{\varphi}^{++}(P_f, q_{f\perp}) \frac{\not{P}_f}{M_f} L_r \Gamma^\mu \varphi^{++}(P, q_\perp) \right],\tag{3.18}$$

where

$$L_r = \frac{(M_f - \tilde{\omega}_{1f} - \tilde{\omega}_{2f})}{(P_{fP} - \omega_{1f} - \omega_2)} \Lambda_1^+(p_{1f\perp}).\tag{3.19}$$

Here we use the relativistic wave function for a 0^- meson, which has the form

$$\varphi_{0^-}(q_\perp) = M \left[\frac{\not{P}}{M} \varphi_1(q_\perp) + \varphi_2(q_\perp) + \frac{\not{q}_\perp}{M} \varphi_3(q_\perp) + \frac{\not{P}\not{q}_\perp}{M^2} \varphi_4(q_\perp) \right] \gamma_5, \quad (3.20)$$

where the radial wave functions $\varphi_1 \sim \varphi_4$ fulfill the constraint conditions

$$\begin{aligned} \varphi_3 &= \frac{M(\omega_2 - \omega_1)}{m_1\omega_2 + m_2\omega_1} \varphi_2, \\ \varphi_4 &= -\frac{M(\omega_1 + \omega_2)}{m_1\omega_2 + m_2\omega_1} \varphi_1. \end{aligned} \quad (3.21)$$

The numerical values of φ_1 and φ_2 can be obtained by solving the Salpeter equation.

For the 1^- state, the relativistic wave function has the form

$$\begin{aligned} \varphi_{1^-}(q_\perp) &= (q_\perp \cdot \epsilon) \left[f_1(q_\perp) + \frac{\not{P}}{M} f_2(q_\perp) + \frac{\not{q}_\perp}{M} f_3(q_\perp) + \frac{\not{P}\not{q}_\perp}{M^2} f_4(q_\perp) \right], \\ &+ M \not{\epsilon} \left[f_5(q_\perp) + \frac{\not{P}}{M} f_6(q_\perp) + \frac{\not{q}_\perp}{M} f_7(q_\perp) + \frac{\not{P}\not{q}_\perp}{M^2} f_8(q_\perp) \right]. \end{aligned} \quad (3.22)$$

And the radial wave functions $f_1 \sim f_8$ fulfill the constraint conditions

$$\begin{aligned} f_1(q_\perp) &= \frac{q_\perp^2 f_3(\omega_1 + \omega_2) + 2M^2 f_5 \omega_2}{M(m_1\omega_2 + m_2\omega_1)}, \\ f_2(q_\perp) &= \frac{q_\perp^2 f_4(\omega_1 - \omega_2) + 2M^2 f_6 \omega_2}{M(m_1\omega_2 + m_2\omega_1)}, \\ f_7(q_\perp) &= \frac{M(\omega_1 - \omega_2)}{m_1\omega_2 + m_2\omega_1} f_5, \\ f_8(q_\perp) &= \frac{M(\omega_1 + \omega_2)}{m_1\omega_2 + m_2\omega_1} f_6. \end{aligned} \quad (3.23)$$

For comparison, we also present the non-relativistic forms of the wave functions, which have the form

$$\varphi_{0^-}(q_\perp) = M \left[\frac{\not{P}}{M} \varphi_1(q_\perp) + \varphi_2(q_\perp) \right] \gamma_5 \quad (3.24)$$

and

$$\varphi_{1^-}(q_\perp) = M \not{\epsilon} \left[f_3(q_\perp) + \frac{\not{P}}{M} f_4(q_\perp) \right] \quad (3.25)$$

for the 0^- and 1^- mesons, respectively.

4 Numerical Results and Discussions

In this work, we use the Cornell potential as the interaction kernel [49], which is a linear scalar potential plus a vector interaction potential

$$\begin{aligned} V(\vec{q}) &= V_s(\vec{q}) + V_v(\vec{q}) \gamma_0 \otimes \gamma^0, \\ V_s(\vec{q}) &= -\left(\frac{\lambda}{\alpha} + V_0 \right) \delta^3(\vec{q}) + \frac{\lambda}{\pi^2} \frac{1}{(\vec{q}^2 + \alpha^2)^2}, \\ V_v(\vec{q}) &= -\frac{2}{3\pi^2} \frac{\alpha_s(\vec{q})}{(\vec{q}^2 + \alpha^2)}, \end{aligned} \quad (4.1)$$

where the QCD running coupling constant $\alpha_s(\vec{q}) = \frac{12\pi}{33-2N_f} \frac{1}{\log(a+\vec{q}^2/\Lambda_{QCD}^2)}$ is used; the symbol \otimes denotes that the Salpeter wave function is sandwiched between the two γ^0 matrices. The constants λ, α, a, V_0 and Λ_{QCD} are the parameters characterizing the potential, which have the values [50],

$$\begin{aligned} a = e = 2.7183, \quad \alpha = 0.060 \text{ GeV}, \quad \lambda = 0.210 \text{ GeV}^2, \\ m_u = 0.305 \text{ GeV}, \quad m_d = 0.311 \text{ GeV}, \quad m_s = 0.500 \text{ GeV}, \\ m_c = 1.62 \text{ GeV}, \quad m_b = 4.96 \text{ GeV}, \quad \Lambda_{QCD} = 0.270 \text{ GeV}. \end{aligned} \quad (4.2)$$

In addition, the CKM matrix element $|V_{cb}| = 0.0411$ from PDG [22] is also used.

Since the Salpeter equations of the 0^- and 1^- mesons have been solved in our previous paper [49, 51], we will not show the details, but directly give the numerical results of wave functions. With Eq.(2.2) and Eq.(2.4), we can get the form factors of $\bar{B}^0 \rightarrow D^+ e \bar{\nu}_e$, $\bar{B}^0 \rightarrow D^{*+} e \bar{\nu}_e$ and $B_c \rightarrow \eta_c(J/\psi) e \bar{\nu}_e$ which are presented in Fig.2, Fig.3 and Fig.4, respectively. In each figure, we plot two diagrams, the left one is for the case when the final state is a pseudoscalar, and the right one for the vector final state.

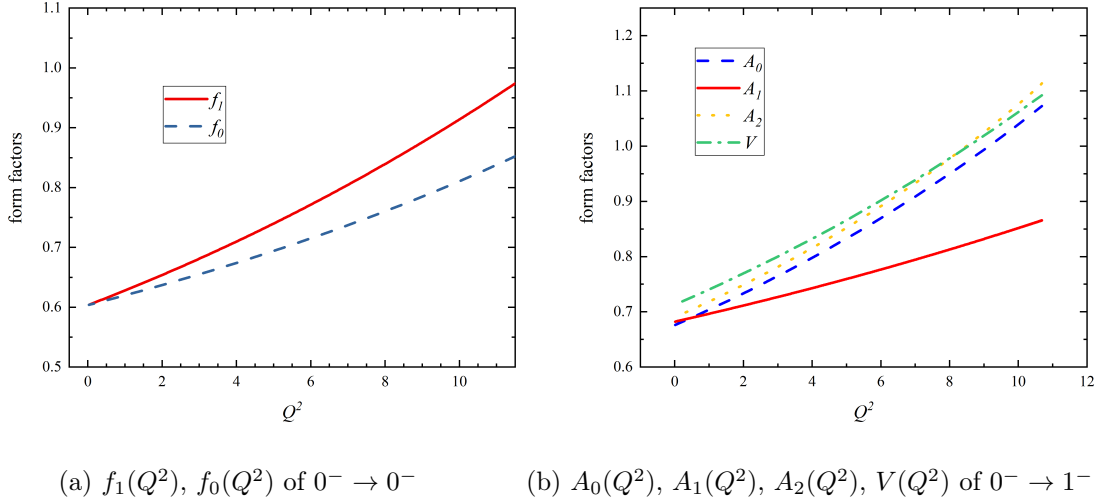


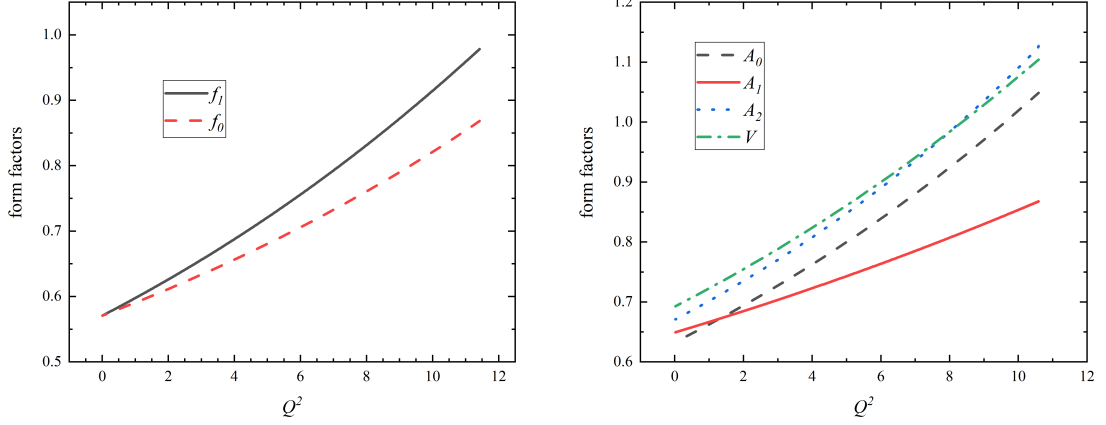
Figure 2: The form factors of decays $\bar{B}^0 \rightarrow D^{(*)+} e \bar{\nu}_e$.

To check our result, we compare it with that achieved by other method, where the form factors are parameterized in a different way. According to Ref. [3], The differential width can be written as

$$\frac{d\Gamma(B \rightarrow D \ell \bar{\nu}_\ell)}{dw} = \frac{G_F^2 m_D^3}{48\pi^3} (m_B + m_D)^2 (w^2 - 1)^{3/2} \eta_{EW}^2 \mathcal{G}^2(w) |V_{cb}|^2, \quad (4.3)$$

where the factor $\eta_{EW} = 1 + \alpha/\pi \ln M_Z/m_B \simeq 1.0066$ takes into account the short distance QED corrections. Moreover, the recoil variable w is defined as the product of the 4-velocities of the B and D mesons, which is related to Q^2 by the formula

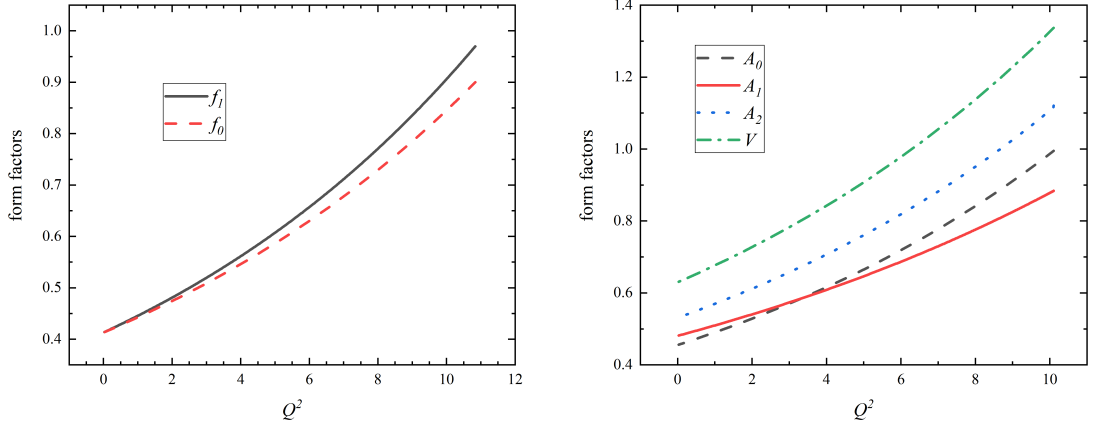
$$w = v_B \cdot v_D = \frac{m_B^2 + m_D^2 - Q^2}{2m_B m_D}. \quad (4.4)$$



(a) $f_1(Q^2)$, $f_0(Q^2)$ of $0^- \rightarrow 0^-$

(b) $A_0(Q^2)$, $A_1(Q^2)$, $A_2(Q^2)$, $V(Q^2)$ of $0^- \rightarrow 1^-$

Figure 3: The form factors of decays $B_s^0 \rightarrow D_s^{(*)+} e \bar{\nu}_e$.



(a) $f_1(Q^2)$, $f_0(Q^2)$ of $0^- \rightarrow 0^-$

(b) $A_0(Q^2)$, $A_1(Q^2)$, $A_2(Q^2)$, $V(Q^2)$ of $0^- \rightarrow 1^-$

Figure 4: The form factors of decays $B_c^- \rightarrow \eta_c(J/\psi) e \bar{\nu}_e$.

For the decay process $B^0 \rightarrow D^- \ell \bar{\nu}_\ell$, we can get [52]

$$\begin{aligned} \mathcal{G}(z) &= \frac{2\sqrt{r}}{(1+r)} f_1(w) \\ &= \mathcal{G}(1) (1 - 8\rho^2 z + (51\rho^2 - 10) z^2 - (252\rho^2 - 84) z^3), \end{aligned} \quad (4.5)$$

where

$$z(w) = \frac{\sqrt{w+1} - \sqrt{2}}{\sqrt{w+1} + \sqrt{2}}. \quad (4.6)$$

Here we have defined $r = m_D/m_B$. If the lepton mass can be neglected, the differential decay rate will not depend on $f_0(w)$. Then we can express the form factors of channel

$\bar{B}^0 \rightarrow D^+ e \bar{\nu}_e$ as the functions of w , which is show in Fig.5(a). In Fig.5(b), we compare our result of f_1 with the experimental data [52], to show the uncertainty of the input parameters. We vary all the model parameters simultaneously around their center values within $\pm 10\%$ and take the largest uncertainty as the errors. Within theoretical uncertainties, our results consist with Belle's data.

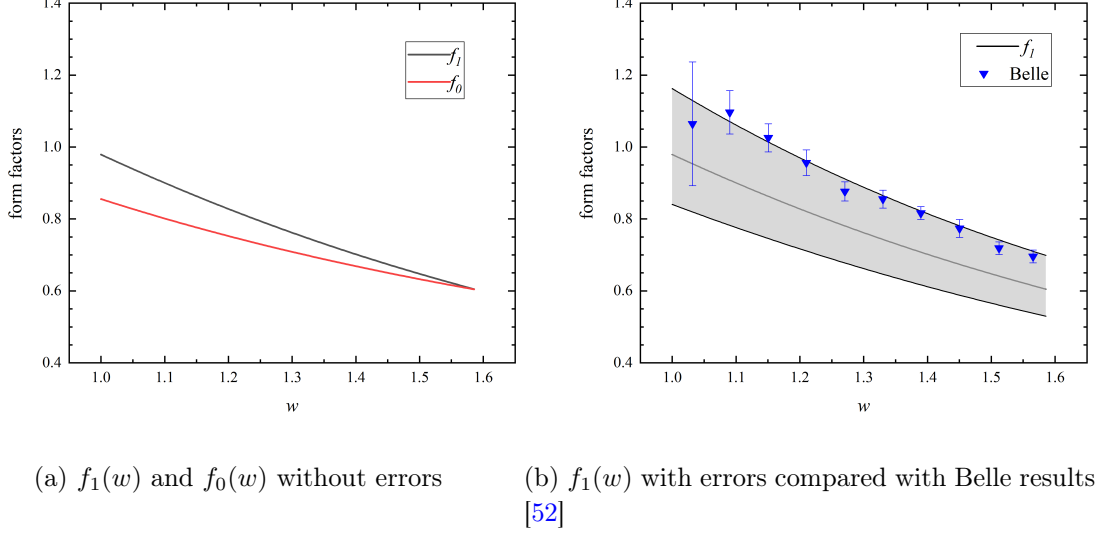


Figure 5: The form factors with and without errors of the decay $\bar{B}^0 \rightarrow D^+ e \bar{\nu}_e$.

$\mathcal{G}(1)$ and ρ^2 are independent parameters which describe respectively the normalization and the shape of the measured decay distributions. Using Eq. (4.5) and the numerical values of form factors as well as $|V_{cb}| = 41.1 \times 10^{-3}$ from PDG [22], we obtain the values of $\mathcal{G}(1)$ and the slope ρ^2 which are shown in table 1, where the average of experimental data and LQCD's results are also given as comparison. For both parameters, our results are smaller than the experimental data. However, considering the uncertainties, they are still consistent with each other. The normalization parameter $\mathcal{G}(1)$ and the slope ρ^2 for other semileptonic decays of B_q meson to the pseudoscalar are shown in table 2.

Table 1: The normalization and the slope of $B^0 \rightarrow D^- \ell \nu_\ell$.

parameters	$\eta_{EW} \mathcal{G}(1) V_{cb} [10^{-3}]$	ρ^2
ours	$35.6^{+4.9}_{-5.0}$	0.97 ± 0.16
Averages of EX [3]	$41.57 \pm 0.45_{\text{stat}} \pm 0.89_{\text{syst}}$	$1.128 \pm 0.024_{\text{stat}} \pm 0.023_{\text{syst}}$
LQCD [33]	$42.81(40)$	$1.119(71)$

For the decay process $\bar{B}^0 \rightarrow D^{*+} \ell \bar{\nu}_\ell$, where the final meson is a vector, we can get a similar formula as that of the pseudoscalar case [34]

$$\frac{d\Gamma(\bar{B}^0 \rightarrow D^{*+} \ell \bar{\nu}_\ell)}{dw} = \frac{G_F^2 m_{D^*}^3}{48\pi^3} (m_B - m_{D^*})^2 \eta_{EW}^2 \chi(w) \mathcal{F}^2(w) |V_{cb}|^2, \quad (4.7)$$

Table 2: The normalization and the slope of B^- , B_s and B_c decays to a pseudoscalar meson.

Channel	$\eta_{\text{EW}}\mathcal{G}(1) V_{cb} [10^{-3}]$	ρ^2
$B^- \rightarrow D^0 e \nu_e$	$35.5^{+4.6}_{-4.8}$	0.96 ± 0.13
$B_s \rightarrow D_s e \nu_e$	$35.9^{+4.5}_{-4.7}$	1.13 ± 0.21
$B_c \rightarrow \eta_c e \nu_e$	$37.4^{+4.8}_{-4.2}$	2.64 ± 0.23

where

$$\begin{aligned} \chi(w)\mathcal{F}^2(w) = & h_{A_1}^2(w)\sqrt{w^2-1}(w+1)^2 \left\{ 2 \left[\frac{1-2wr+r^2}{(1-r)^2} \right] \left[1 + R_1^2(w) \frac{w^2-1}{w+1} \right] + \right. \\ & \left. \left[1 + (1-R_2(w)) \frac{w-1}{1-r} \right]^2 \right\}, \end{aligned} \quad (4.8)$$

and

$$h_{A_1}(w) = \frac{2\sqrt{m_B m_{D^*}}}{m_B + m_{D^*}} \frac{A_1(Q^2)}{1 - \frac{Q^2}{(m_B + m_{D^*})^2}}. \quad (4.9)$$

Here we use the parametrization of form factors introduced by Caprini, Lellouch and Neubert (CLN) [53]

$$\begin{aligned} h_{A_1}(w) &= h_{A_1}(1) [1 - 8\rho^2 z + (53\rho^2 - 15)z^2 - (231\rho^2 - 91)z^3], \\ R_1(w) &= \frac{h_V(w)}{h_{A_1}(w)} \approx 1.27 - 0.12(w-1) + 0.05(w-1)^2, \\ R_2(w) &= \frac{h_{A_3}(w) + r h_{A_2}(w)}{h_{A_1}(w)} \approx 0.80 + 0.11(w-1) - 0.06(w-1)^2. \end{aligned} \quad (4.10)$$

All these functions, $h_{A_1}(w)$, $R_1(w)$, $R_2(w)$ etc., are alterations of the former form factors, which can be obtained by using Eq. (2.12). For example, at zero recoil, where $w = 1$, $z = 0$ and $Q^2 = Q_{\text{max}}^2 = (m_B + m_D)^2$, we have

$$\mathcal{F}(1) = h_{A_1}(1) = \frac{m_B + m_{D^*}}{2\sqrt{m_B m_{D^*}}} A_1(Q_{\text{max}}^2). \quad (4.11)$$

We will not show details of other functions, but present the the results of $\eta_{\text{EW}}\mathcal{F}(1)|V_{cb}|$, ρ^2 , $R_1(1)$ and $R_2(1)$ in table 3, where the LQCD results and the averages of experimental data are also listed for comparison. Similarly, in table 4, the normalization $\mathcal{G}(1)$ and the slope ρ^2 of the other $0^- \rightarrow 1^-$ channels are shown.

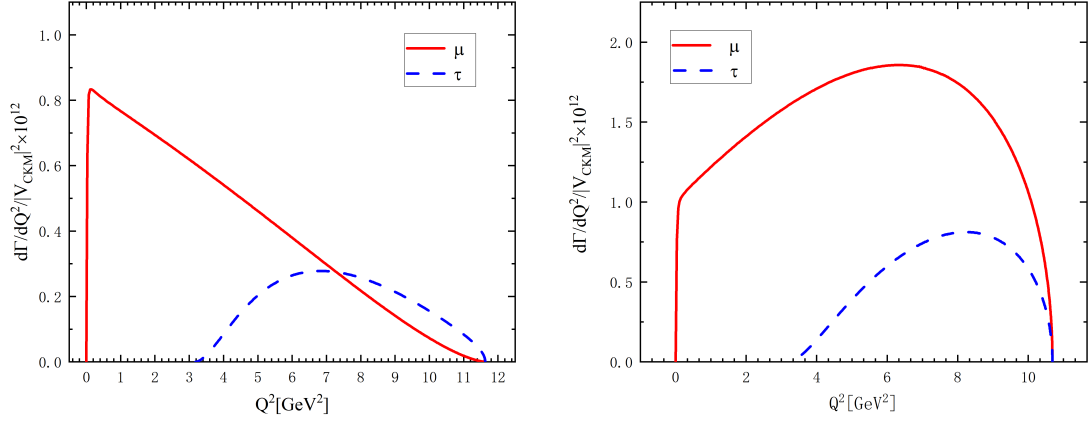
The differential branching fraction is another observable. With the numerical values of form factors calculated by the improved BS method, we straightforwardly obtain differential branching fractions. In Fig.6(a), the spectra of $B \rightarrow D\mu\nu$ and $B \rightarrow D\tau\nu$ are shown. In Fig.6(b), the spectra for $B \rightarrow D^*\mu\nu$ and $B \rightarrow D^*\tau\nu$ are given. Our results of differential branching fractions for the cases of $B \rightarrow D$ agree very well with those of Ref. [34] by the lattice QCD method. In Fig.7 and Fig.8, we present respectively the differential branching fractions for B_s and B_c decays.

Table 3: The normalization and the slope of $B^0 \rightarrow D^{*-}\ell\nu_\ell$.

parameters	$\eta_{EW}\mathcal{F}(1) V_{cb} [10^{-3}]$	ρ^2
ours	$40.06^{+4.98}_{-4.13}$	1.04 ± 0.19
Averages of EX [3]	$35.61 \pm 0.11_{\text{stat}} \pm 0.41_{\text{syst}}$	$1.205 \pm 0.015_{\text{stat}} \pm 0.021_{\text{syst}}$
LQCD [34]	$36.71 \pm 0.41 \pm 0.84$	$1.29(17)$
parameters	$R_1(1)$	$R_2(1)$
ours	$1.55^{+0.12}_{-0.11}$	$0.98^{+0.12}_{-0.11}$
LQCD [34]	1.404 ± 0.032	0.854 ± 0.020

Table 4: The normalization and the slope of B^- , B_s and B_c decay to a vector meson.

Channel	$\eta_{EW}\mathcal{F}(1) V_{cb} [10^{-3}]$	ρ^2	$R_1(1)$	$R_2(1)$
$B^- \rightarrow D^{*0}e\nu_e$	$40.1^{+4.9}_{-4.2}$	1.04 ± 0.18	$1.55^{+0.11}_{-0.12}$	$0.98^{+0.12}_{-0.11}$
$B_s \rightarrow D_s^*e\nu_e$	$39.8^{+4.6}_{-4.4}$	1.18 ± 0.15	$1.34^{+0.10}_{-0.11}$	$1.03^{+0.15}_{-0.14}$
$B_c \rightarrow J/\psi e\nu_e$	$38.8^{+4.8}_{-4.1}$	2.67 ± 0.16		



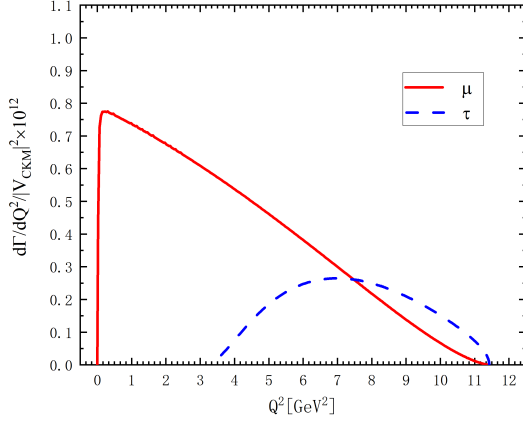
(a) The spectrum for $B \rightarrow D\mu(\tau)\nu$

(b) The spectrum for $B \rightarrow D^*\mu(\tau)\nu$

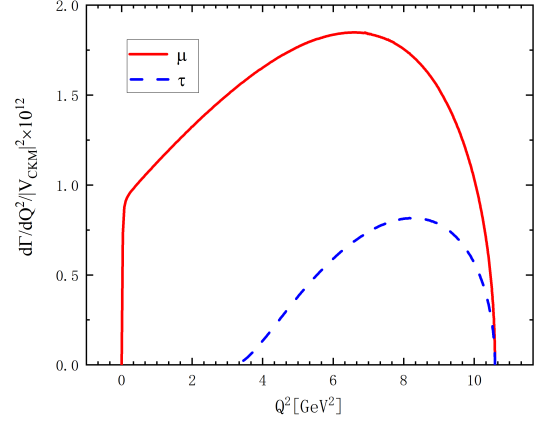
Figure 6: The differential branching fractions for B meson decays.

For completeness, we also calculate the angular distribution $d\Gamma/d\cos\theta$, where θ is the angle between \vec{P}_f (the momentum of the final meson) and \vec{P}_l^* (the momentum of the charged lepton in the center-of-momentum frame of $l^-\bar{\nu}_l$). The results are presented in Fig. 9, Fig.10, and Fig.11. Moreover, we can also study the the lepton spin asymmetry and the forward-backward asymmetry, which are defined respectively as

$$A_\lambda^P(Q^2) = \frac{d\Gamma[\lambda_\ell = -1/2]/dQ^2 - d\Gamma[\lambda_\ell = 1/2]/dQ^2}{d\Gamma[\lambda_\ell = -1/2]/dQ^2 + d\Gamma[\lambda_\ell = 1/2]/dQ^2}, \quad (4.12)$$

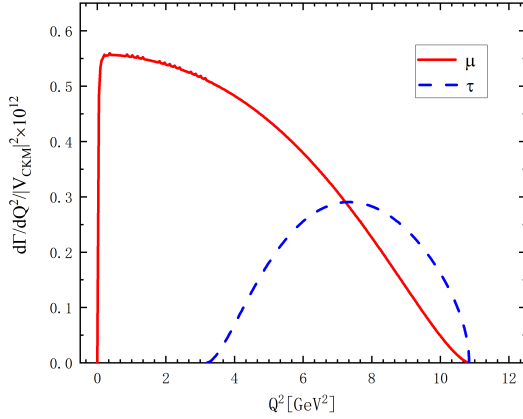


(a) The spectrum for $B_s \rightarrow D_s \mu(\tau) \nu$

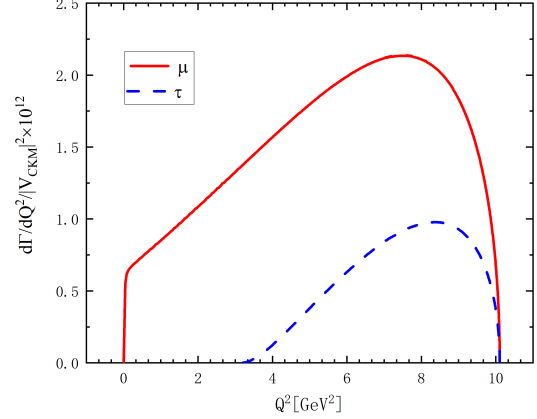


(b) The spectrum for $B_s \rightarrow D_s^* \mu(\tau) \nu$

Figure 7: The differential branching fractions for B_s meson decays.



(a) The spectrum for $B_c \rightarrow \eta_c \mu(\tau) \nu$



(b) The spectrum for $B_c \rightarrow J/\psi \mu(\tau) \nu$

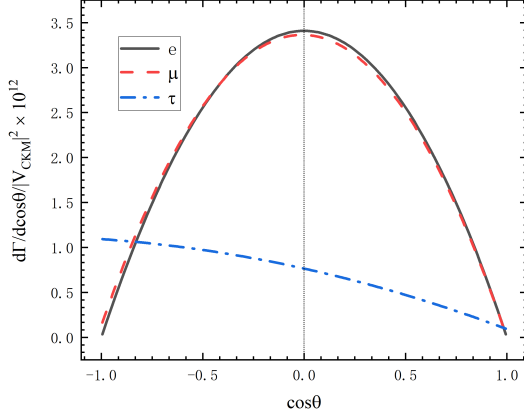
Figure 8: The differential branching fractions for B_c meson decays.

and

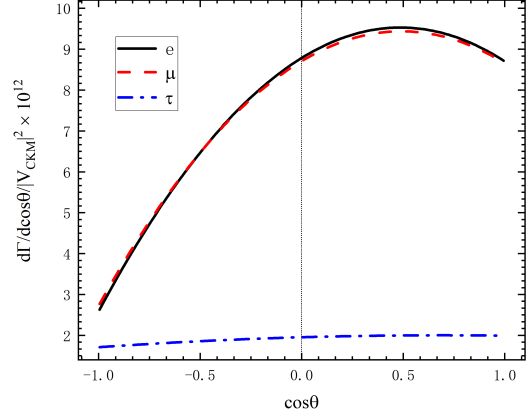
$$A_{\cos\theta}^P(Q^2) = \frac{\int_{-1}^0 d\cos\theta \left(\frac{d^2\Gamma}{dQ^2 d\cos\theta} \right) - \int_0^1 d\cos\theta \left(\frac{d^2\Gamma}{dQ^2 d\cos\theta} \right)}{d^2\Gamma/dQ^2}. \quad (4.13)$$

The results are shown in Fig.12 ~ Fig.17.

Finally, the decay widths and corresponding branching ratios by the improved BS method are shown in table 5 and table 6, where table 5 is the cases of B_q decays to a pseudoscalar and table 6 is for the cases of B_q to a vector. As before, the errors are calculated by varying all the parameters around their center values within $\pm 10\%$.

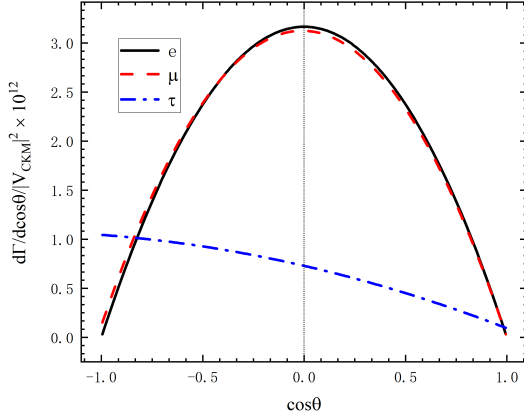


(a) The spectrum for $B \rightarrow D\ell\nu_\ell$

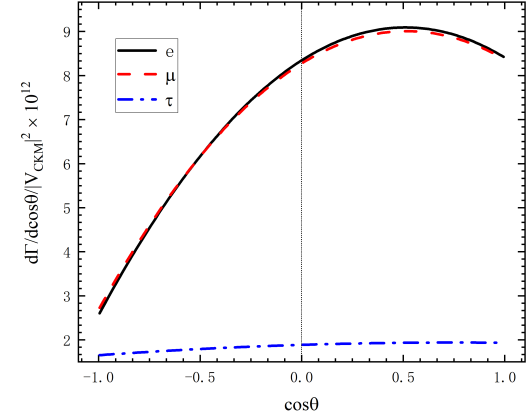


(b) The spectrum for $B \rightarrow D^*\ell\nu_\ell$

Figure 9: The angular distributions for B meson decays.



(a) The spectrum for $B_s \rightarrow D_s\ell\nu_\ell$

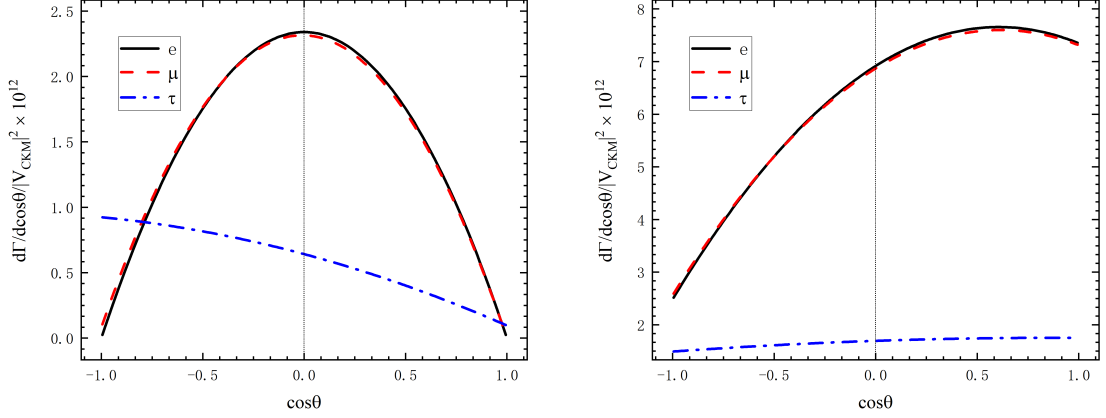


(b) The spectrum for $B_s \rightarrow D_s^*\ell\nu_\ell$

Figure 10: The angular distributions for B_s meson decays.

In table 5 and table 6, for comparison, we also show other theoretical results as well as the experimental data from PDG. In the last column of table 5, we show our results of the ratios $R(D)$, $R(D_s)$ and $R(\eta_c)$. And the corresponding vector cases $R(D^*)$, $R(D_s^*)$ and $R(J/\psi)$ are shown in the last column of table 6. From these two tables, we can see that, our results of branching ratios consist with experimental data within errors. However, for the $B^- \rightarrow D^0$ processes, we get a larger value of $R(D)$ than the experimental data. Because the center value of the branching ratio of $B^- \rightarrow D^0 e \nu_e$ is smaller than that of experimental data, while for the $B^- \rightarrow D^0 \tau \nu_\tau$ process, the result is opposite.

To compare with each other, we give the table 7, in which we show the ratios of $R(D)$,



(a) The spectrum for $B_c \rightarrow \eta_c \ell \nu_\ell$

(b) The spectrum for $B_c \rightarrow J/\psi \ell \nu_\ell$

Figure 11: The angular distributions for B_c meson decays.

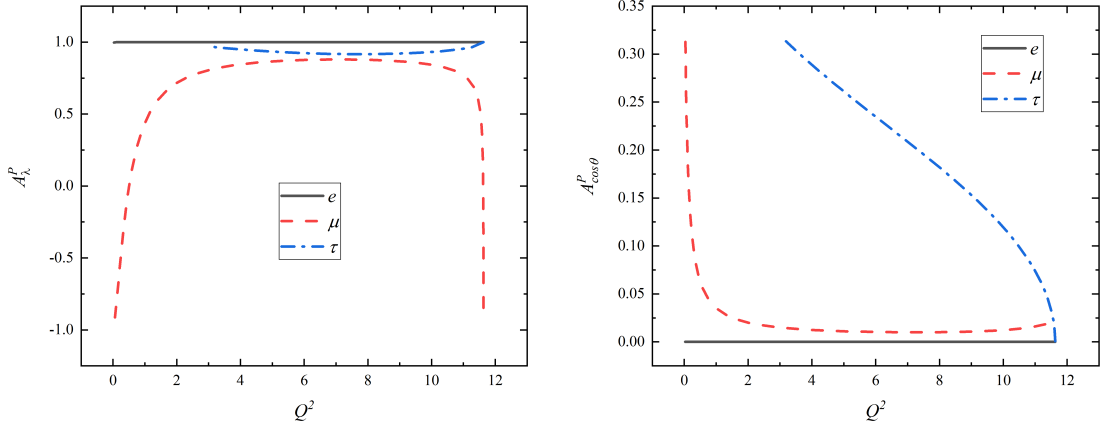


Figure 12: A_λ^P (left) and $A_{\cos\theta}^P$ (right) of the decay $\bar{B}^0 \rightarrow D^+(1S) \ell \nu_\ell$.

$R(D^{(*)})$ and $R(J/\psi)$ by this method, other SM predictions and experimental data. There are many theoretical predictions of the SM available now, while we only present few of them in this paper for comparison. We can see that, though we have relative large theoretical uncertainties in the branching ratios, we get very small uncertainties in the ratios of $R(D)$, $R(D^{(*)})$ and $R(J/\psi)$, as most of the uncertainties are cancelled. This also happens in other theoretical predictions. Our result of $R(D)$ is close to other SM predictions, while larger than experimental data except the recent Belle data in 2019. For $R(D^{(*)})$, most theoretical results are consistent with each other, but smaller than the experimental data. For $R(J/\psi)$, the theoretical predictions of the SM is much smaller than the experimental data.

In conclusion, we give a relativistic calculation of the ratios $R(D)$, $R(D^*)$ and $R(J/\psi)$ using the instantaneous BS method which has been improved to provide a more covari-

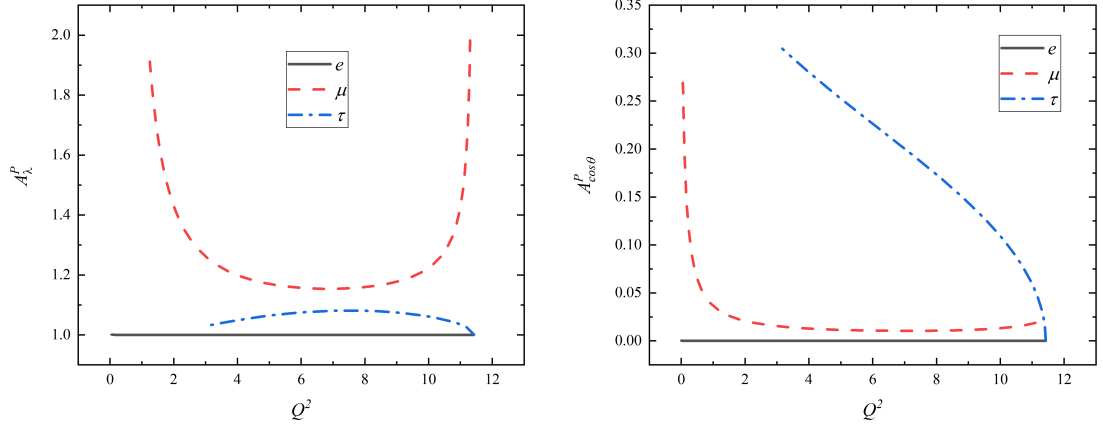


Figure 13: A_λ^P (left) and $A_{\cos\theta}^P$ (right) of the decay $\bar{B}_s^0 \rightarrow D_s^+(1S)\ell\nu_\ell$.

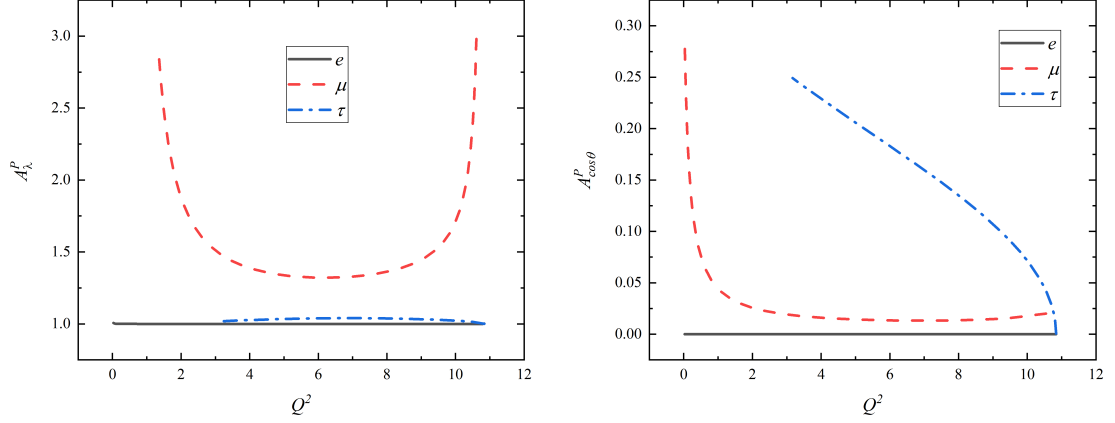


Figure 14: A_λ^P (left) and $A_{\cos\theta}^P$ (right) of the decay $B_c^- \rightarrow \eta_c \ell \nu_\ell$.

ant formula to calculate the transition matrix element. Within errors, our results of the branching fractions are consistent with the experimental data. However, their ratios $R(D)$, $R(D^*)$ and $R(J/\psi)$, which are consistent with other theoretical predictions, are distinctly different from the experimental data except the recent Belle result [45].

Acknowledgments

This work was supported in part by the National Natural Science Foundation of China (NSFC) under Grant Nos. 11575048, 11405037, 11505039. We also thank the HEPC Studio at Physics School of Harbin Institute of Technology for access to computing resources through INSPUR-HPC@hepc.hit.edu.cn.

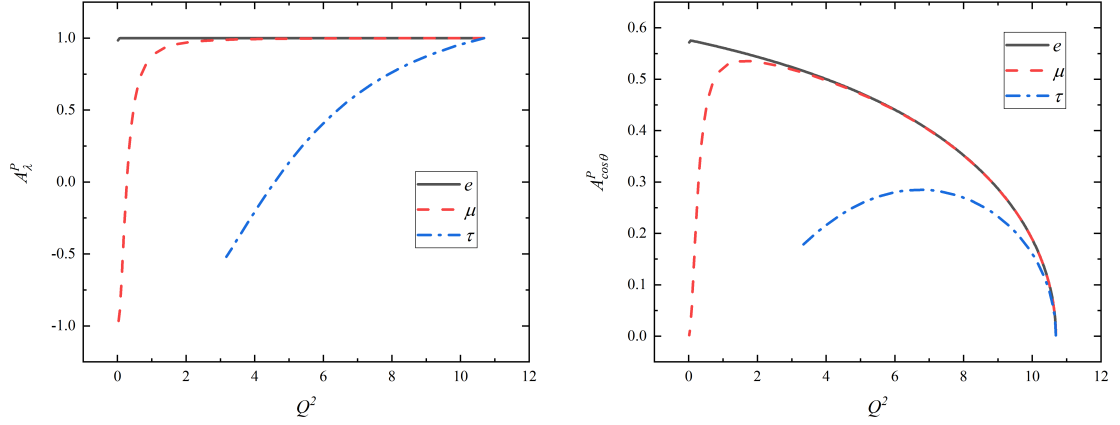


Figure 15: A_{λ}^P (left) and $A_{\cos\theta}^P$ (right) of the decay $\bar{B}^0 \rightarrow D^{*+} \ell \nu_{\ell}$

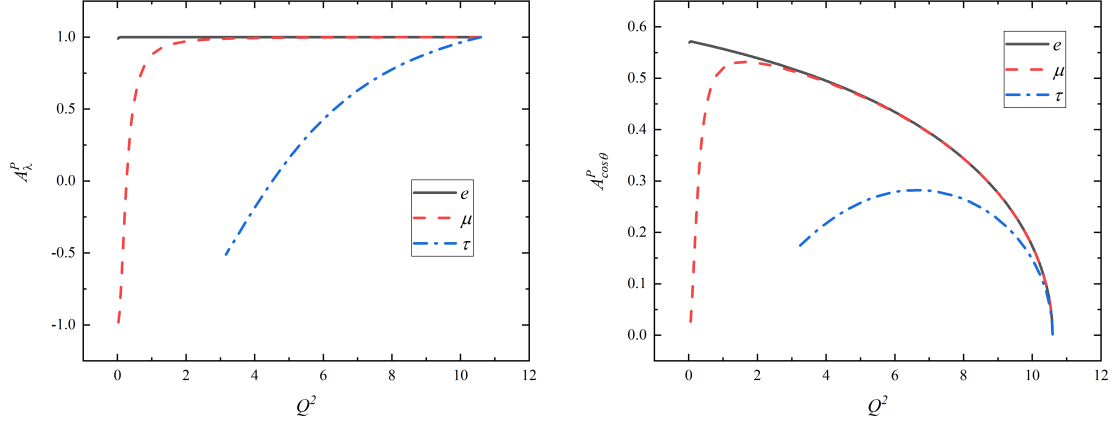


Figure 16: A_{λ}^P (left) and $A_{\cos\theta}^P$ (right) of the decay $\bar{B}_s^0 \rightarrow D_s^{*+}(1S) \ell \nu_{\ell}$.

References

- [1] Y. Li and C.-D. Lü, *Recent Anomalies in B Physics*, *Sci. Bull.* **63** (2018) 267.
- [2] ATLAS, CMS, LHCb collaboration, *Flavour anomalies: a review*, *J. Phys. Conf. Ser.* **1137** (2019) 012025.
- [3] HFLAV collaboration, *Averages of b-hadron, c-hadron, and τ -lepton properties as of summer 2016*, *Eur. Phys. J.* **C77** (2017) 895 [[1612.07233](#)].
- [4] S. Fajfer, J. F. Kamenik, I. Nisandzic and J. Zupan, *Implications of Lepton Flavor Universality Violations in B Decays*, *Phys. Rev. Lett.* **109** (2012) 161801 [[1206.1872](#)].
- [5] S. Sahoo, R. Mohanta and A. K. Giri, *Explaining the R_K and $R_{D^{(*)}}$ anomalies with vector leptoquarks*, *Phys. Rev.* **D95** (2017) 035027 [[1609.04367](#)].
- [6] S. Fajfer, J. F. Kamenik and I. Nisandzic, *On the $B \rightarrow D^* \tau \bar{\nu}_{\tau}$ Sensitivity to New Physics*,

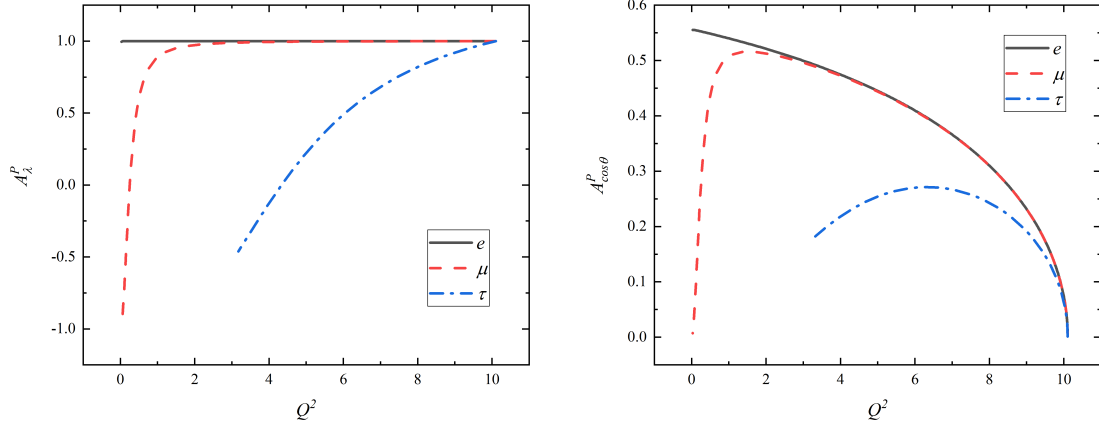


Figure 17: A_λ^P (left) and $A_{\cos\theta}^P$ (right) of the decay $B_c^- \rightarrow J/\psi \ell \nu_\ell$.

Table 5: Decay widths (10^{-15} GeV), branching ratios (%) and $R(D)$.

Channels	width	Br	Br [32]	Br [30, 31]	Br (PDG [22])	Ratio (τ/ℓ)
$B^- \rightarrow D^0 e \nu_e$	$7.68^{+2.67}_{-1.84}$	$1.91^{+0.67}_{-0.45}$	2.20 – 3.00	1.50 – 2.40	2.20 ± 0.10	$0.312^{+0.006}_{-0.007}$
$B^- \rightarrow D^0 \mu \nu_\mu$	$7.65^{+2.65}_{-1.83}$	$1.91^{+0.66}_{-0.45}$			2.20 ± 0.10	$0.313^{+0.006}_{-0.007}$
$B^- \rightarrow D^0 \tau \nu_\tau$	$2.40^{+0.77}_{-0.54}$	$0.60^{+0.20}_{-0.13}$			0.77 ± 0.25	
$\bar{B}^0 \rightarrow D^+ e \nu_e$	$7.65^{+2.67}_{-1.83}$	$1.77^{+0.62}_{-0.42}$	2.20 – 3.00	1.30 – 2.20	2.20 ± 0.10	$0.312^{+0.006}_{-0.006}$
$\bar{B}^0 \rightarrow D^+ \mu \nu_\mu$	$7.64^{+2.66}_{-1.84}$	$1.76^{+0.62}_{-0.42}$			2.20 ± 0.10	$0.313^{+0.006}_{-0.007}$
$\bar{B}^0 \rightarrow D^+ \tau \nu_\tau$	$2.39^{+0.77}_{-0.54}$	$0.55^{+0.18}_{-0.12}$			1.03 ± 0.22	
$\bar{B}_s^0 \rightarrow D_s^+ e \nu_e$	$7.12^{+2.73}_{-1.84}$	$1.64^{+0.63}_{-0.42}$	2.80 – 3.80			$0.320^{+0.009}_{-0.009}$
$\bar{B}_s^0 \rightarrow D_s^+ \mu \nu_\mu$	$7.10^{+2.73}_{-1.83}$	$1.63^{+0.63}_{-0.42}$				$0.321^{+0.009}_{-0.009}$
$\bar{B}_s^0 \rightarrow D_s^+ \tau \nu_\tau$	$2.28^{+0.80}_{-0.54}$	$0.52^{+0.18}_{-0.12}$				
$B_c^- \rightarrow \eta_c e \nu_e$	$5.25^{+2.68}_{-1.80}$	$0.40^{+0.21}_{-0.14}$	0.45 [44]	0.50 [54]		$0.384^{+0.032}_{-0.042}$
$B_c^- \rightarrow \eta_c \mu \nu_\mu$	$5.25^{+2.69}_{-1.79}$	$0.40^{+0.21}_{-0.14}$				$0.384^{+0.033}_{-0.041}$
$B_c^- \rightarrow \eta_c \tau \nu_\tau$	$2.02^{+0.77}_{-0.55}$	$0.15^{+0.06}_{-0.04}$				

Phys. Rev. D **D85** (2012) 094025 [[1203.2654](#)].

- [7] U. Nierste, S. Trine and S. Westhoff, *Charged-Higgs effects in a new $B \rightarrow D\tau\nu$ differential decay distribution*, *Phys. Rev. D* **D78** (2008) 015006.
- [8] A. Datta, M. Duraisamy and D. Ghosh, *Diagnosing New Physics in $b \rightarrow c\tau\nu_\tau$ decays in the light of the recent BaBar result*, *Phys. Rev. D* **D86** (2012) 034027.
- [9] D. Bečirević, N. Košnik and A. Tayduganov, *$\bar{B} \rightarrow D\tau\bar{\nu}_\tau$ vs. $\bar{B} \rightarrow D\mu\bar{\nu}_\mu$* , *Phys. Lett. B* **B716** (2012) 208.
- [10] A. Crivellin, C. Greub and A. Kokulu, *Explaining $B \rightarrow D\tau\nu$, $B \rightarrow D^*\tau\nu$ and $B \rightarrow \tau\nu$ in a 2HDM of type III*, *Phys. Rev. D* **D86** (2012) 054014.
- [11] M. Bauer and M. Neubert, *Minimal Leptoquark Explanation for the $R_{D^{(*)}}$, R_K , and*

Table 6: Decay widths (10^{-14} GeV), branching ratios (%) and $R(D^*)$.

Channels	width	Br	Br [32]	Br [30, 31]	Br (PDG [22])	Ratio(τ/ℓ)
$B^- \rightarrow D^{*0} e \nu_e$	$2.62^{+0.75}_{-0.55}$	$6.54^{+1.88}_{-1.37}$	$5.90 - 7.60$	$4.36 - 8.94$	4.88 ± 0.10	$0.249^{+0.001}_{-0.002}$
$B^- \rightarrow D^{*0} \mu \nu_\mu$	$2.61^{+0.75}_{-0.55}$	$6.51^{+1.88}_{-1.36}$			4.88 ± 0.10	$0.249^{+0.001}_{-0.002}$
$B^- \rightarrow D^{*0} \tau \nu_\tau$	$0.65^{+0.18}_{-0.13}$	$1.63^{+0.48}_{-0.33}$			1.88 ± 0.20	
$\bar{B}^0 \rightarrow D^{*+} e \nu_e$	$2.61^{+0.75}_{-0.55}$	$6.03^{+1.74}_{-1.26}$	$5.90 - 7.60$	$4.57 - 9.12$	4.88 ± 0.10	$0.248^{+0.001}_{-0.002}$
$\bar{B}^0 \rightarrow D^{*+} \mu \nu_\mu$	$2.60^{+0.75}_{-0.54}$	$6.01^{+1.74}_{-1.25}$			4.88 ± 0.10	$0.249^{+0.001}_{-0.002}$
$\bar{B}^0 \rightarrow D^{*+} \tau \nu_\tau$	$0.65^{+0.18}_{-0.13}$	$1.50^{+0.42}_{-0.30}$			1.67 ± 0.13	
$\bar{B}_s^0 \rightarrow D_s^{*+} e \nu_e$	$2.50^{+0.78}_{-0.55}$	$5.74^{+1.79}_{-1.27}$		$1.89 - 6.61$	$2.80 - 3.80$	$0.251^{+0.002}_{-0.003}$
$\bar{B}_s^0 \rightarrow D_s^{*+} \mu \nu_\mu$	$2.48^{+0.78}_{-0.55}$	$5.71^{+1.79}_{-1.26}$				$0.252^{+0.002}_{-0.003}$
$\bar{B}_s^0 \rightarrow D_s^{*+} \tau \nu_\tau$	$0.63^{+0.19}_{-0.13}$	$1.44^{+0.43}_{-0.31}$				
$B_c^- \rightarrow J/\psi e \nu_e$	$2.11^{+0.78}_{-0.56}$	$1.62^{+0.60}_{-0.43}$	1.36 [44]	1.67 [54]		$0.267^{+0.009}_{-0.011}$
$B_c^- \rightarrow J/\psi \mu \nu_\mu$	$2.10^{+0.77}_{-0.55}$	$1.62^{+0.59}_{-0.43}$				$0.268^{+0.009}_{-0.012}$
$B_c^- \rightarrow J/\psi \tau \nu_\tau$	$0.56^{+0.18}_{-0.13}$	$0.43^{+0.14}_{-0.10}$				

Table 7: The experiment data and SM prediction of $R(D)$, $R(D^*)$ and $R(J/\psi)$ with the result in this paper.

experiment	$R(D)$	$R(D^*)$	$R(J/\psi)$
ours	$0.312^{+0.006}_{-0.007}$	$0.248^{+0.001}_{-0.002}$	$0.267^{+0.008}_{-0.012}$
Lattice QCD [34]	0.300 ± 0.008		
Heavy quark expansion [6]		0.252 ± 0.003	
LCSR [29]		$0.260(8)$	
CCQM [27]			0.24
BarBar [3]	$0.440 \pm 0.058 \pm 0.042$	$0.332 \pm 0.024 \pm 0.018$	
Belle (2017) [3]	$0.375 \pm 0.058 \pm 0.042$	$0.293 \pm 0.038 \pm 0.015$	
Belle (2019) [45]	$0.307 \pm 0.037 \pm 0.016$	$0.283 \pm 0.018 \pm 0.014$	
LHCb [3, 25]		$0.285 \pm 0.019 \pm 0.029$	$0.71 \pm 0.17 \pm 0.18$

$(g-2)_g$ Anomalies, *Phys. Rev. Lett.* **116** (2016) 141802.

- [12] I. Doršner, S. Fajfer, A. Greljo, J. F. Kamenik and N. Košnik, *Physics of leptoquarks in precision experiments and at particle colliders*, *Phys. Rept.* **641** (2016) 1.
- [13] A. Celis, M. Jung, X.-Q. Li and A. Pich, *Scalar contributions to $b \rightarrow c(u)\tau\nu$ transitions*, *Phys. Lett.* **B771** (2017) 168.
- [14] BABAR collaboration, *Evidence for an excess of $\bar{B} \rightarrow D^{(*)}\tau^-\bar{\nu}_\tau$ decays*, *Phys. Rev. Lett.* **109** (2012) 101802.
- [15] BABAR collaboration, *Measurement of an Excess of $\bar{B} \rightarrow D^{(*)}\tau^-\bar{\nu}_\tau$ Decays and Implications for Charged Higgs Bosons*, *Phys. Rev.* **D88** (2013) 072012.
- [16] BELLE collaboration, *Measurement of the branching ratio of $\bar{B} \rightarrow D^{(*)}\tau^-\bar{\nu}_\tau$ relative to $\bar{B} \rightarrow D^{(*)}\ell^-\bar{\nu}_\ell$ decays with hadronic tagging at Belle*, *Phys. Rev.* **D92** (2015) 072014.

- [17] BELLE collaboration, *Measurement of the branching ratio of $\bar{B}^0 \rightarrow D^{*+}\tau^-\bar{\nu}_\tau$ relative to $\bar{B}^0 \rightarrow D^{*+}\ell^-\bar{\nu}_\ell$ decays with a semileptonic tagging method*, *Phys. Rev.* **D94** (2016) 072007.
- [18] BELLE collaboration, *Measurement of the τ lepton polarization and $R(D^*)$ in the decay $\bar{B} \rightarrow D^*\tau^-\bar{\nu}_\tau$* , *Phys. Rev. Lett.* **118** (2017) 211801.
- [19] LHCb collaboration, *Measurement of the ratio of branching fractions $\mathcal{B}(\bar{B}^0 \rightarrow D^{*+}\tau^-\bar{\nu}_\tau)/\mathcal{B}(\bar{B}^0 \rightarrow D^{*+}\mu^-\bar{\nu}_\mu)$* , *Phys. Rev. Lett.* **115** (2015) 111803.
- [20] LHCb collaboration, *Measurement of the ratio of the $B^0 \rightarrow D^{*-}\tau^+\nu_\tau$ and $B^0 \rightarrow D^{*-}\mu^+\nu_\mu$ branching fractions using three-prong τ -lepton decays*, *Phys. Rev. Lett.* **120** (2018) 171802.
- [21] LHCb collaboration, *Test of Lepton Flavor Universality by the measurement of the $B^0 \rightarrow D^{*-}\tau^+\nu_\tau$ branching fraction using three-prong τ decays*, *Phys. Rev.* **D97** (2018) 072013 [[1711.02505](#)].
- [22] PARTICLE DATA GROUP collaboration, *Review of Particle Physics*, *Phys. Rev.* **D98** (2018) 030001.
- [23] D. Bigi and P. Gambino, *Revisiting $B \rightarrow D\ell\nu$* , *Phys. Rev.* **D94** (2016) 094008.
- [24] S. Aoki et al., *Review of lattice results concerning low-energy particle physics*, *Eur. Phys. J.* **C77** (2017) 112 [[1607.00299](#)].
- [25] LHCb collaboration, *Measurement of the ratio of branching fractions $\mathcal{B}(B_c^+ \rightarrow J/\psi\tau^+\nu_\tau)/\mathcal{B}(B_c^+ \rightarrow J/\psi\mu^+\nu_\mu)$* , *Phys. Rev. Lett.* **120** (2018) 121801.
- [26] R. Watanabe, *New Physics effect on $B_c \rightarrow J/\psi\tau\bar{\nu}$ in relation to the $R_{D^{(*)}}$ anomaly*, *Phys. Lett.* **B776** (2018) 5.
- [27] C.-T. Tran, M. A. Ivanov, J. G. Körner and P. Santorelli, *Implications of new physics in the decays $B_c \rightarrow (J/\psi, \eta_c)\tau\nu$* , *Phys. Rev.* **D97** (2018) 054014.
- [28] S. Bhattacharya, S. Nandi and S. Kumar Patra, *$b \rightarrow c\tau\nu_\tau$ Decays: a catalogue to compare, constrain, and correlate new physics effects*, *Eur. Phys. J.* **C79** (2019) 268.
- [29] D. Bigi, P. Gambino and S. Schacht, *$R(D^*)$, $|V_{cb}|$, and the Heavy Quark Symmetry relations between form factors*, *JHEP* **11** (2017) 061 [[1707.09509](#)].
- [30] K. Azizi, *QCD Sum Rules Study of the Semileptonic $B_{(s)}(B^\pm)(B^0) \rightarrow D_{(s)}(1968)(D^0)(D^\pm)\ell\nu$ Decays*, *Nucl. Phys.* **B801** (2008) 70.
- [31] K. Azizi and M. Bayar, *Semileptonic $B_{(q)} \rightarrow D^*(q)\ell\nu(q = s, d, u)$ Decays in QCD Sum Rules*, *Phys. Rev.* **D78** (2008) 054011.
- [32] A. D. Polosa, *The CQM model*, *Riv. Nuovo Cim.* **23N11** (2000) 1 [[hep-ph/0004183](#)].
- [33] HPQCD collaboration, *$B \rightarrow D\ell\nu$ form factors at nonzero recoil and extraction of $|V_{cb}|$* , *Phys. Rev.* **D92** (2015) 054510.
- [34] HPQCD collaboration, *Lattice QCD calculation of the $B_{(s)} \rightarrow D_{(s)}^*\ell\nu$ form factors at zero recoil and implications for $|V_{cb}|$* , *Phys. Rev.* **D97** (2018) 054502.
- [35] M. Jung and D. M. Straub, *Constraining new physics in $b \rightarrow c\ell\nu$ transitions*, *JHEP* **01** (2019) 009.
- [36] W.-F. Wang, Y.-Y. Fan and Z.-J. Xiao, *Semileptonic decays $B_c \rightarrow (\eta_c, J/\Psi)\ell\nu$ in the perturbative QCD approach*, *Chin. Phys.* **C37** (2013) 093102.
- [37] V. V. Kiselev, *Exclusive decays and lifetime of B_c meson in QCD sum rules*, [hep-ph/0211021](#).

- [38] H.-B. Fu, L. Zeng, W. Cheng, X.-G. Wu and T. Zhong, *Longitudinal leading-twist distribution amplitude of the J/ψ meson within the background field theory*, *Phys. Rev.* **D97** (2018) 074025.
- [39] T. Zhong, Y. Zhang, X.-G. Wu, H.-B. Fu and T. Huang, *The ratio $\mathcal{R}(D)$ and the D -meson distribution amplitude*, *Eur. Phys. J.* **C78** (2018) 937.
- [40] R. Zhu, Y. Ma, X.-L. Han and Z.-J. Xiao, *Relativistic corrections to the form factors of B_c into S -wave Charmonium*, *Phys. Rev.* **D95** (2017) 094012.
- [41] J.-M. Shen, X.-G. Wu, H.-H. Ma and S.-Q. Wang, *QCD corrections to the B_c to charmonia semileptonic decays*, *Phys. Rev.* **D90** (2014) 034025.
- [42] W. Wang, Y.-L. Shen and C.-D. Lu, *Covariant Light-Front Approach for $B_{(c)}$ transition form factors*, *Phys. Rev.* **D79** (2009) 054012.
- [43] E. Hernandez, J. Nieves and J. M. Verde-Velasco, *Study of exclusive semileptonic and non-leptonic decays of B_c - in a nonrelativistic quark model*, *Phys. Rev.* **D74** (2006) 074008.
- [44] D. Ebert, R. N. Faustov and V. O. Galkin, *Weak decays of the B_c meson to charmonium and D mesons in the relativistic quark model*, *Phys. Rev.* **D68** (2003) 094020.
- [45] BELLE collaboration, *Measurement of $\mathcal{R}(D)$ and $\mathcal{R}(D^*)$ with a semileptonic tagging method*, [1904.08794](#).
- [46] Z.-H. Wang, G.-L. Wang, H.-F. Fu and Y. Jiang, *The Strong Decays of Orbitally Excited B_{sJ}^* Mesons by Improved Bethe-Salpeter Method*, *Phys. Lett.* **B706** (2012) 389.
- [47] H.-F. Fu, Y. Jiang, C. S. Kim and G.-L. Wang, *Probing Non-leptonic Two-body Decays of B_c meson*, *JHEP* **06** (2011) 015.
- [48] C.-H. Chang, J.-K. Chen and G.-L. Wang, *Instantaneous formulation for transitions between two instantaneous bound states and its gauge invariance*, *Commun. Theor. Phys.* **46** (2006) 467.
- [49] C. S. Kim and G.-L. Wang, *Average kinetic energy of heavy quark ($\mu^2(\pi)$) inside heavy meson of 0^- state by Bethe-Salpeter method*, *Phys. Lett.* **B584** (2004) 285.
- [50] T. Wang, G.-L. Wang, Y. Jiang and W.-L. Ju, *Electromagnetic Decay of $X(3872)$ as the $1^1D_2(2^-)$ charmonium*, *J. Phys.* **G40** (2013) 035003.
- [51] G.-L. Wang, *Decay constants of heavy vector mesons in relativistic Bethe-Salpeter method*, *Phys. Lett.* **B633** (2006) 492.
- [52] BELLE collaboration, *Measurement of the decay $B \rightarrow D\ell\nu_\ell$ in fully reconstructed events and determination of the Cabibbo-Kobayashi-Maskawa matrix element $|V_{cb}|$* , *Phys. Rev.* **D93** (2016) 032006.
- [53] I. Caprini, L. Lellouch and M. Neubert, *Dispersive bounds on the shape of $B \rightarrow D^{(*)}$ lepton anti-neutrino form-factors*, *Nucl. Phys.* **B530** (1998) 153.
- [54] M. A. Ivanov, J. G. Korner and P. Santorelli, *Exclusive semileptonic and nonleptonic decays of the B_c meson*, *Phys. Rev.* **D73** (2006) 054024.